

Not All Symbols Are Equal: Importance-Aware Constellation Design for Semantic Communication

Albert Shaju*, Christo Kurisummoottil Thomas*, and Mayukh Roy Chowdhury†

* Department of Electrical and Computer Engineering, Worcester Polytechnic Institute, Worcester, MA, USA.

† Nokia Bell Labs, Bengaluru, India.

Emails:ashaju@wpi.edu,cthomas2@wpi.edu,mayukh.roy_chowdhury@nokia-bell-labs.com

Abstract—Semantic communication systems for goal-oriented transmission must protect task-relevant information not only through source compression but also via physical layer mapping. Existing approaches decouple constellation design and semantic encoding, exposing critical symbols to channel errors at the same rate as irrelevant ones. Contrary to this, in this paper, a joint semantic-physical layer framework is proposed, which is composed of a vector quantized-variational autoencoder that extracts discrete latent concepts, a semantic criticality indicator (SCI) that scores each concept by task relevance, and a deep reinforcement learning agent that dynamically selects the transmission subset based on instantaneous channel conditions. At the physical layer, a learned semantic-aware M -QAM constellation assigns symbol positions according to joint co-occurrence statistics and SCI scores, departing from the uniform spacing and Gray coding of standard M -QAM which minimizes average BER without regard for semantic content. We introduce a novel semantic symbol vulnerability (SSV) metric and a semantic protection probability (SPP) to quantify the exposure of task-critical symbols to decoding errors, and prove that any Gray-coded constellation is strictly suboptimal in SCI-Weighted SSV whenever the source exhibits non-uniform semantic importance and co-occurrence statistics. Simulation results demonstrate that the proposed constellation achieves near 100% SPP across modulation orders from 4-QAM to 1024-QAM versus 50% for standard constellations at high spectral efficiency, a 21:1 compression ratio with semantic quality above 0.9, generalizing across MNIST, Fashion-MNIST, and FSDD without modification.

I. INTRODUCTION

The design of wireless communication systems has historically optimized bit-level fidelity, while being agnostic to the meaning carried by transmitted bits. While this is theoretically justified under Shannon’s framework for general sources [1], it becomes bandwidth inefficient when the RX only intends to perform inference on the received messages. *Semantic communication (SC)* [2] and [3] addresses this by jointly optimizing source representation and transmission schemes to maximize downstream task performance rather than reconstruction fidelity. Recent advances in deep learning have enabled end-to-end learned SC systems that directly map source data to transmitted signals. Vector quantized-variational autoencoders (VQ-VAE) [4] produce compact discrete representations suitable for digital transmission, and reinforcement learning (RL) agents have demonstrated the ability to adaptively rate-control semantic payloads in response to channel state. However, these application layer level advances have not been matched by equivalent progress at the physical layer (PHY) modulation stage. Once semantic concepts are compressed and selected, they are typically either transmitted

as continuous analog signals over learned channel mappings, foregoing compatibility with standard digital infrastructure, or mapped to Gray-coded constellations that optimize average bit error rate (BER) uniformly with no consideration for which symbols carry semantically critical information.

Parallel to SC, the authors of [5] and [6] pioneered the view of a communication system as an autoencoder, jointly optimizing transmitter (TX) and receiver (RX) for minimum block error rate and demonstrating that learned constellations can outperform standard QAM for specific channels. However, all prior learned constellation work [5]–[7] optimizes for average BER uniformly across all symbols, with no mechanism to differentiate protection or adapt information rates based on the semantic importance of individual concept indices. Importance-aware transmission has been studied at the resource allocation level, where deep reinforcement learning (DRL)-based schemes adaptively assign bandwidth and quantization bits based on semantic relevance [8] and [9], and task-oriented rate control has been explored using information bottleneck principles [10]. Unequal error protection for semantic features has been proposed via proactive importance-ordered restructuring [11], prioritizing transmission of critical features. In contrast to these approaches, which operate at the source or scheduling layer and leave the physical constellation unchanged, our work is the first to embed semantic importance directly into the constellation assignment itself, closing the gap between semantic-aware source coding and PHY modulation.

The main contribution of this paper is a joint semantic PHY framework that co-designs the constellation assignment with the semantic importance and statistical co-occurrence structure of the learned concept vocabulary. First, we propose a *learned semantic-aware constellation mapper* whose complex symbol coordinates are continuous trainable variables optimized by an *semantic criticality indicator (SCI)*-weighted loss, establishing a direct one-to-one mapping between VQ-VAE concept indices and physical symbols. Second, we introduce the SCI-weighted semantic symbol vulnerability (SSV), and semantic protection probability (SPP) as novel metrics for quantifying the exposure of task-critical symbols to decoding errors and the degree to which a constellation preferentially protects semantically important concepts. Third, we prove that any Gray-coded M -QAM constellation is strictly suboptimal in SCI-Weighted SSV whenever the source exhibits non-uniform semantic importance and co-occurrence statistics, characterize the protection gap in closed form, and establish via corol-

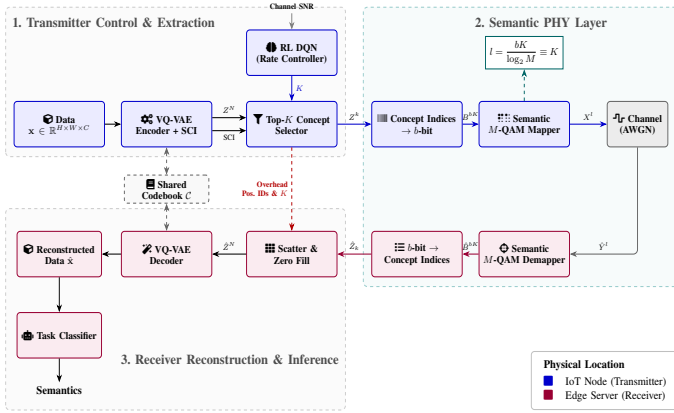


Fig. 1: Overall Architecture of the proposed SC system.

lary the BER-semantic error decoupling observed empirically. Finally, simulation results demonstrate consistently higher semantic quality and compression than standard M -QAM across all modulation orders, near 100% SPPR up to 1024-QAM versus 50% for Gray-coded baselines, generalizing across visual and acoustic domains without modification.

II. PROBLEM FORMULATION AND SYSTEM MODEL

Consider a resource-constrained sensor device, such as a low-power IoT node deployed in an industrial or smart city environment, that acquires multidimensional data $\mathbf{x} \in \mathbb{R}^{H \times W \times C}$, where H , W , and C denote the spatial and feature channel dimensions of the observation, respectively. The node transmits this data over a bandwidth-limited wireless channel to an edge server. The edge server then utilizes a hosted neural inference engine to perform a downstream inference task \mathcal{T} on the reconstructed signal. Unlike a conventional communication link where both endpoints share reconstruction as the objective, the sensor has no inference capability and transmits solely to enable accurate task execution at the server. The sensor operates under a strict transmit power budget P and must minimize the number of transmitted physical symbols ℓ representing \mathbf{x} to reduce both bandwidth consumption and over the air latency. The edge server periodically feeds back the estimated channel SNR to the sensor over a reliable low-rate control channel, enabling adaptive payload selection. We model this feedback as error-free and instantaneous, consistent with standard assumptions in the adaptive modulation literature [12]. The fundamental challenge is therefore to compress the source data into the minimum physical symbols that preserves the semantic content required for accurate inference at the server. This should ensure that the most task-critical features are physically protected against channel impairments at the modulation layer. Crucially, our architecture maintains structural compatibility with conventional PHY setups, enabling seamless integration into existing systems. The architecture of the proposed end-to-end SC system, as shown in Fig. 1, are discussed next.

A. SC Model

1) *Semantic Extraction and Control*: At the TX, a VQ-VAE encoder is adopted because the variational prior regularizes the encoder output distribution ensuring stable and semantically coherent latent representations, while vector quantization

produces a learned discrete codebook \mathcal{C} whose entries are jointly optimized with the encoder and downstream task loss. The encoder maps the input \mathbf{x} to N continuous embeddings $\mathbf{z}_i \in \mathbb{R}^D$, defined collectively as $\mathbf{Z} \in \mathbb{R}^{N \times D}$. Each continuous embedding is quantized to a discrete latent vector $\mathbf{z}_{q,i}$ (collectively as \mathbf{Z}_q) via a nearest-neighbor lookup in \mathcal{C} : $\mathbf{z}_{q,i} = \mathbf{e}_{k^*}$, where $k^* = \underset{k, \text{s.t. } \mathbf{e}_k \in \mathcal{C}}{\operatorname{argmin}} \|\mathbf{z}_i - \mathbf{e}_k\|$, producing the full discrete concept vector $\mathbf{Z}^N \in \mathbb{Z}^N$. A SCI network operates in parallel, assigning each concept a continuous SCI score $I_i \in (0, 1)$. A DRL agent, via a deep Q-network (DQN), observes the SNR fed back from the edge server and selects the optimal transmission subset size $K \leq N$. Top- K concepts and positional IDs are extracted to enable adaptive transmission of essential semantics.

2) *Semantic PHY*: The K selected concept indices are modulated using a learned semantic M -QAM constellation $\mathcal{X} = \{x_1, \dots, x_M\} \subset \mathbb{C}$, where $M = |\mathcal{C}|$ and x_i is the constellation symbol. Setting the codebook size equal to the modulation order establishes a direct one-to-one mapping between each $b = \log_2 M$ -bit concept index and a distinct physical symbol. The constellation coordinates are trainable variables subject to the average power constraint: $\frac{1}{M} \sum_{i=1}^M |x_i|^2 \leq P$. The resulting $\ell = K$ symbols, defined as X^ℓ traverse a wireless channel, yielding received symbols Y^ℓ .

3) *Semantic Reconstruction and Task Execution*: At the edge server, the semantic M -QAM demapper recovers the K concept indices \hat{i} from the noisy received symbol \hat{y} via minimum-distance detection: $\hat{i} = \underset{i \in \{1, \dots, M\}}{\operatorname{argmin}} \|\hat{y} - x_i\|^2$. At the RX, using the shared codebook \mathcal{C} and the control-path Positional IDs, the recovered vectors are scattered back to their original spatial coordinates within an N -slot grid. The remaining $N - K$ unselected positions are zero-filled to yield the reconstructed $\hat{\mathbf{Z}}$. The VQ-VAE decoder reconstructs $\hat{\mathbf{x}}$ from $\hat{\mathbf{Z}}$ and a frozen task classifier \mathcal{T} evaluates the downstream inference on the reconstructed image.

III. PROPOSED AI ARCHITECTURE FOR SEMANTIC PHY

A. Task-Specific Differentiable Classifier

To evaluate semantic quality, we pre-train a lightweight multi-layer perceptron (MLP) classifier \mathcal{T} on clean source images. The network maps the flattened data (\mathbf{x}) vector to a class probability distribution $\hat{\mathbf{p}} \in \mathbb{R}^{|\mathcal{Y}|}$ via two fully connected hidden layers with ReLU activations and dropout regularization, trained to minimize the sparse categorical cross-entropy loss: $\mathcal{L}_{\text{cls}}(y, \hat{\mathbf{p}}) = -\log \hat{p}_y$, where $\hat{p}_y = p(\mathcal{T}(\hat{\mathbf{x}}) = y)$.

B. SCI-Weighted VQ-VAE and SCI

The core compression engine is an SCI-weighted VQ-VAE (S-VQ-VAE) that jointly learns discrete semantic representations and their task relevance. The SCI network is implemented as a two-layer MLP with sigmoid output and requires no explicit importance supervision. Its parameters are trained end-to-end via gradients of \mathcal{L}_{cls} that backpropagate through the decoder and across the quantization step via the straight-through estimator (STE) [13], implicitly forcing higher scores onto concepts whose presence improves downstream classification accuracy.

TABLE I: System Hyperparameters and Simulation Setup

Parameter	Value	Parameter	Value
<i>S-VQ-VAE & SCI Network</i>			
D (Latent Dim)	64	N (Concept Slots)	64
Hidden Units	[512, 256]	Batch Size	128
β (Commit)	0.25	τ (Temp.)	$1.0 \rightarrow 0.1$
λ_{sem}	1.0	Learning Rate	10^{-3}
<i>DQN Rate Controller</i>			
State Dim	2	$ \mathcal{A} $ (Actions)	12
Hidden Units	[64, 64]	γ (Gamma)	0.99
Buffer Size	10^4	ϵ (Epsilon)	$1.0 \rightarrow 0.01$
K_{\min}, K_{\max}	5, 64	Bonus α	0.2
<i>Semantic PHY & Channel</i>			
M -QAM Orders	{4...1024}	Training Steps	4000
Init. Grid	Rect. QAM	SNR Range	$[-10, 20]$ dB
Optimizer	Adam	Learning rate (PHY)	10^{-3}

1) *SCI-Weighted Forward Pass*: For a given K , each continuous embedding z_i is scaled by its normalized SCI weight via element-wise multiplication, High-importance concepts (i.e., concepts with high SCI score) receive near-unit weights and survive codebook quantization faithfully, while low-importance concepts are attenuated toward zero and effectively suppressed. Here, we use a temperature parameter τ to progressively harden the soft selection into a discrete Top- K mask at inference. During inference the soft SCI weighting is replaced by hard Top- K masking.

2) *Two-Phase Training*: Training proceeds in two phases to ensure stable convergence. In *Phase 1*, which is the representation learning, the model trains as a standard VQ-VAE to establish robust reconstruction capability: $\mathcal{L}_{\text{VQ}} = \mathbb{E}[\|\mathbf{x} - \hat{\mathbf{x}}\|_2^2] + \beta \|\text{sg}[\mathbf{Z}_q] - \mathbf{Z}\|_2^2$, where $\text{sg}[\cdot]$ denotes the stop-gradient operator and β is the commitment loss weight. The codebook entries are updated via the exponential moving average of assigned encoder outputs, following the standard VQ-VAE training procedure [4]. In *Phase 2*, called semantic activation, the downstream task loss is activated, reorganizing the codebook geometry around task-relevant features:

$$\mathcal{L}_{\text{total}} = \mathcal{L}_{\text{VQ}} + \lambda_{\text{sem}} \mathcal{L}_{\text{cls}}(y, \hat{\mathbf{x}}), \quad (1)$$

where λ_{sem} is the semantic loss weight. Because the importance weights are applied before quantization, gradients from \mathcal{L}_{cls} backpropagate through the decoder, across the quantization step via the STE, and directly into both the SCI network and the codebook entries, forcing the learned discrete vocabulary to concentrate task-relevant structure into a small subset of actively used codewords.

C. Deep Reinforcement Learning Rate Controller

Adaptive semantic concept selection is formulated as a Markov decision process (MDP) solved by a deep Q-network (DQN) agent. At each transmission interval t , the agent observes state $s_t = \text{SNR}_n$, the channel SNR normalized to $[0, 1]$ from the feedback path described in Section II, and selects action $a_t \equiv K \in \mathcal{A}$, where \mathcal{A} is a discrete set of $|\mathcal{A}|$ uniformly spaced values spanning $[K_{\min}, K_{\max}]$. The reward function is a multi-objective formulation balancing *semantic quality*, *bandwidth efficiency*, and *PHY reliability*:

$$r_t = Q_{\text{task}} + \mathcal{B}_{\text{comp}} + \mathcal{B}_a - \lambda P_e - \mathcal{P}(K), \quad (2)$$

where $Q_{\text{task}} \in [0, 1]$ is the downstream task accuracy, P_e the BER, and $\mathcal{P}(K)$ is a regularization term that penalizes selection of extreme payload sizes $K \in \{K_{\min}, K_{\max}\}$,

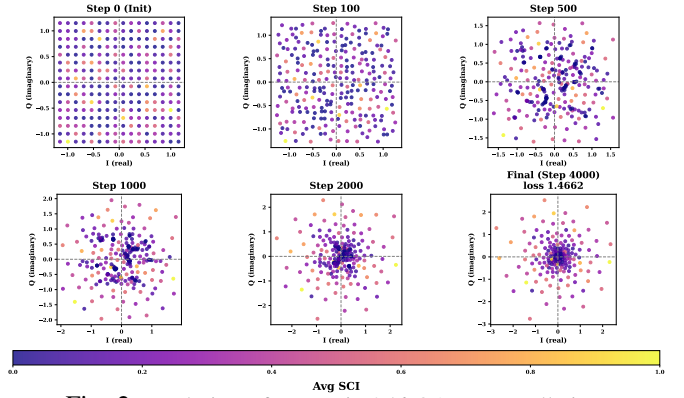


Fig. 2: Evolution of semantic 256-QAM constellation.

preventing the agent from collapsing to a degenerate policy that ignores channel conditions. Two conditional bonuses guide exploration. $\mathcal{B}_{\text{comp}} = \alpha \ln(N/K)$ if $Q_{\text{task}} > Q_0$ and zero otherwise, rewarding compression only when semantic quality is preserved, and \mathcal{B}_a incentivizes fewer concepts at high SNR and more at low SNR to enforce channel-adaptive behavior. The DQN employs an MLP policy network with ϵ -greedy exploration, experience replay, and a periodically synchronized target network for Bellman stability.

D. Learned Semantic M -QAM Constellation

1) *SCI-Weighted Constellation Loss*: Unlike standard QAM, which minimizes average BER without regard to semantics, the proposed mapper optimizes an SCI-weighted loss that penalizes errors on critical symbols more severely:

$$\mathcal{L}_{\text{QAM}} = -\frac{1}{N_{\text{sym}}} \sum_{j=1}^{N_{\text{sym}}} I_j \log \left(\frac{\exp(-\|\hat{y}_j - x_{y_j}\|^2/N_0)}{\sum_{i=1}^M \exp(-\|\hat{y}_j - x_i\|^2/N_0)} \right), \quad (3)$$

where \hat{y}_j is the received noisy symbol for the j -th transmission, x_{y_j} is the constellation point for true concept index y_j , N_0 is the noise variance, and I_j is the normalized SCI score of the j -th transmitted symbol. By scaling the cross-entropy penalties to decoding errors on high-importance symbols, driving their constellation points toward regions of maximum physical separation from co-occurring neighbors. Training SNR is randomized across $[\text{SNR}_{\min}, \text{SNR}_{\max}]$ at every step to ensure robustness across diverse channel conditions.

2) *Evolution of the Semantic Aware Constellation*: To empirically validate this geometric adaptation, we visualize the optimization trajectory of a 256-QAM constellation for MNIST data in Fig. 2. The constellation initializes as a standard rectangular grid and evolves under the SCI-weighted loss into a task-aware geometry. Symbols carrying low-importance concepts naturally cluster in the dense interior of the I/Q plane, sacrificing their decodability to recover geometric space within the power constraint. Consequently, semantically critical symbols are pushed toward the outer perimeter, maximizing their physical separation and directly validating the spatial isolation strategy proved in Theorem 1. As evident from Fig. 2, only a distinct subset of physical symbols carries high semantic weight for any given class. This sparse physical importance matrix acts as the driving

mathematical force behind the geometric evolution observed in Fig. 2, pushing these specific high-value symbols toward the noise-resilient regions of the constellation.

E. Deployment Considerations

The proposed system follows a strict offline training paradigm. The S-VQ-VAE, SCI, semantic constellation, and DRL agent are trained jointly on a central server prior to deployment. At deployment, the lightweight encoder and SCI MLP are loaded once onto the sensor node, while the learned constellation is distributed as a static lookup table of M complex I/Q coordinates, incurring negligible sharing overhead. The DRL agent handles channel and SNR fluctuations dynamically at inference time, so retraining is not required for channel variation. Retraining is only necessary if the source data distribution shifts fundamentally, as the learned semantic vocabulary of the VQ-VAE codebook would no longer align with the new task context. Architectural details and training hyperparameters are listed in Table I.

IV. OPTIMALITY ANALYSIS OF SEMANTIC CONSTELLATION DESIGN

A. Semantic Symbol Vulnerability Metrics

Evaluating the robustness of semantically critical payloads at the PHY requires moving beyond traditional bit-level error metrics. A decoding error occurs when channel noise displaces a transmitted symbol across a Voronoi boundary into a neighboring region. However, such errors are not equally consequential: errors on symbols encoding task-critical concepts can disrupt downstream inference, while others may have negligible impact. Standard BER treats all errors uniformly, making it a poor metric for semantic robustness. We therefore introduce a metric that weights physical vulnerability by semantic importance and co-occurrence structure.

Definition 1. The *SCI-weighted SSV* (\mathcal{S}_w) of constellation \mathcal{X} quantifies the expected physical vulnerability of semantically critical symbols to decoding errors, weighting each symbol's proximity to its co-occurring neighbors by its average SCI score \bar{I}_i and joint co-occurrence probability $P(i, j)$:

$$\mathcal{S}_w = \frac{1}{M} \sum_{i \in \mathcal{X}} \bar{I}_i \underbrace{\left[M^2 \sum_{j \neq i} P(i, j) \exp(-\|x_i - x_j\|^2) \right]}_{\mathcal{S}_i}. \quad (4)$$

Here, the M^2 scaling ensures fair comparison across modulation orders as joint probabilities shrink with increasing M .

Under complex AWGN, the pairwise error probability between symbols i and j satisfies: $\Pr[\hat{i} = j \mid x_i \text{ sent}] \leq \frac{1}{2} \exp\left(-\frac{\|x_i - x_j\|^2}{4\sigma^2}\right)$, obtained by projecting the complex noise onto the direction $x_j - x_i$ and applying the standard Q-function bound. The exponential decay kernel $\exp(-\|x_i - x_j\|^2)$ used in the \mathcal{S}_w metric of (4) and the pairwise error bound are both strictly decreasing functions of $\|x_i - x_j\|^2$ with identical gradient directions. Their gradients with respect to x_i can be shown to be proportional to $(x_i - x_j)$ with strictly negative scalar prefactors, so they point in identical directions for all $x_i \neq x_j$ and at any fixed SNR. Since this directional equivalence holds for each symbol pair (i, j) independently,

it extends to the $P(i, j)$ -weighted sum in \mathcal{S}_i : minimizing \mathcal{S}_w induces the same optimal symbol placement as minimizing the P -weighted pairwise error probability at any fixed SNR, making \mathcal{S}_w a SNR-agnostic proxy for PHY semantic vulnerability. Crucially, symbols in $\mathcal{N}_i^c = \{j : P(i, j) = 0\}$ contribute zero to \mathcal{S}_i regardless of physical distance, capturing the *probabilistic isolation* effect: channel confusions between mutually exclusive symbols cause no semantic degradation. Finally, we define $\delta_i = \bar{I}_i - \frac{1}{M} \sum_{i=1}^M \bar{I}_i$ and the *SCI score concentration* as $\delta = \max_i \delta_i$. Let $\mathcal{S}_{\text{top}} = \{i : \delta_i > 0\}$ denote the set of symbols with above-average SCI scores. This means that a symbol belongs to \mathcal{S}_{top} if and only if it contributes positively to δ . Further, the *SPP* \mathcal{S}_p measures the fraction of these symbols whose individual vulnerability is strictly below the global mean vulnerability $\mu_S = \frac{1}{M} \sum_i \mathcal{S}_i$:

$$\mathcal{S}_p = \frac{1}{|\mathcal{S}_{\text{top}}|} \sum_{i \in \mathcal{S}_{\text{top}}} \mathbf{1}(\mathcal{S}_i < \mu_S). \quad (5)$$

Operationally, it represents the empirical probability that a semantically critical symbol, if chosen uniformly at random, is shielded better than the constellation average. Further, we formalize the *co-occurrence asymmetry* as $\gamma = \max_{i,j} P(i, j) - \min_{i,j} P(i, j) \geq 0$. When $\delta = 0$ all concepts have equal SCI scores; when $\gamma = 0$ all concept pairs co-occur with equal probability.

Theorem 1. Let \mathcal{X}_{QAM} be a standard Gray-coded M -QAM constellation with average power P , and let \mathcal{X}^* be the \mathcal{S}_w -minimizing constellation over all configurations in \mathbb{C}^M subject to $\frac{1}{M} \sum_i |x_i|^2 \leq P$. If $\delta > 0$ and $\gamma > 0$, then $\mathcal{S}_w(\mathcal{X}^*) < \mathcal{S}_w(\mathcal{X}_{\text{QAM}})$, with protection gap $\Delta_w = \mathcal{S}_w(\mathcal{X}_{\text{QAM}}) - \mathcal{S}_w(\mathcal{X}^*)$ lower-bounded by

$$\Delta_w \geq \frac{\delta \cdot \gamma \cdot M}{1 + \zeta^*/w_{\text{max}}} [\exp(-d_{\text{min}}^2) - \exp(-d_{\text{max}}^2)], \quad (6)$$

where d_{min} is the minimum inter-symbol distance of \mathcal{X}_{QAM} , d_{max} is the maximum feasible inter-symbol distance under power P , $w_{\text{max}} = \max_{i,j} (\bar{I}_i + \bar{I}_j)P(i, j)$, and ζ^* is the Lagrange multiplier of the optimal solution.

Proof Sketch: The \mathcal{S}_w minimisation over \mathbb{C}^M with power constraint admits the Lagrangian $\mathcal{L} = \mathcal{S}_w(\mathcal{X}) + \zeta(\frac{1}{M} \sum_i |x_i|^2 - P)$. Using $P(i, j) = P(j, i)$, the KKT stationarity condition at \mathcal{X}^* is

$$\frac{2\zeta^*}{M} x_i^* = 2 \sum_{j \in \mathcal{N}_i} w_{ij}^* (x_i^* - x_j^*), \quad (7)$$

where $w_{ij}^* = (\bar{I}_i + \bar{I}_j)P(i, j) \exp(-\|x_i^* - x_j^*\|^2)$ and the sum runs only over \mathcal{N}_i since $w_{ij}^* = 0$ for $j \in \mathcal{N}_i^c$. The entire power budget for symbol i is therefore directed toward separating it from its semantically coupled neighbors, with zero budget wasted on non-co-occurring neighbors. For (7) to hold at \mathcal{X}_{QAM} , the weights w_{ij} must be symmetric under all symmetry operations of the rectangular grid, requiring uniform w_{ij} across all nearest-neighbor pairs. Since $\delta > 0$, the importance values \bar{I}_i are non-uniform, and since $\gamma > 0$, the co-occurrence probabilities $P(i, j)$ are non-uniform. Since Gray coding assigns symbol positions independently of \bar{I}_i and $P(i, j)$, the products $(\bar{I}_i + \bar{I}_j)P(i, j)$ are non-uniform across nearest-neighbor pairs, violating the uniformity condition.

Therefore $\nabla_{x_{i^\dagger}} \mathcal{S}_w|_{\mathcal{X}_{\text{QAM}}} \neq \mathbf{0}$ for at least one symbol i^\dagger , and \mathcal{X}_{QAM} is not a stationary point of \mathcal{L} . Since \mathcal{X}_{QAM} is not stationary, there exists a perturbation \mathcal{X}_ϵ feasible under the power constraint such that $\mathcal{S}_w(\mathcal{X}_\epsilon) < \mathcal{S}_w(\mathcal{X}_{\text{QAM}})$. Since \mathcal{X}^* globally minimizes \mathcal{S}_w over the feasible set: $\mathcal{S}_w(\mathcal{X}^*) \leq \mathcal{S}_w(\mathcal{X}_\epsilon) < \mathcal{S}_w(\mathcal{X}_{\text{QAM}})$. Since $\delta > 0$, there exists $i^\dagger = \arg \max_i \bar{I}_i$ with $\bar{I}_{i^\dagger} \geq \mu_{\bar{I}} + \delta$. Since $\gamma > 0$, there exists a pair (i^\dagger, j^\dagger) with $P(i^\dagger, j^\dagger) \geq \gamma/M^2$ after M^2 normalisation. Since Gray coding places symbols independently of co-occurrence structure, this pair is separated by at most d_{\min} on the uniform grid. The monotone decay of the exponential kernel gives the contribution of this pair to $\mathcal{S}_w(\mathcal{X}_{\text{QAM}})$ as at least $(\mu_{\bar{I}} + \delta) \cdot \gamma \cdot \exp(-d_{\min}^2)$. Summing over all M symbols with the M prefactor:

$$\mathcal{S}_w(\mathcal{X}_{\text{QAM}}) \geq \delta \cdot \gamma \cdot M \cdot \exp(-d_{\min}^2).$$

At \mathcal{X}^* , the power constraint bounds $|x_i^*|^2 \leq MP$, so the maximum feasible inter-symbol distance is $d_{\max} = 2\sqrt{MP}$. The KKT force balance in (7) shows that the effective separation scales as $w_{\max}/(w_{\max} + \zeta^*/M)$, yielding the factor $1/(1 + \zeta^*/w_{\max})$. At maximum separation d_{\max} :

$$\mathcal{S}_w(\mathcal{X}^*) \leq \frac{\delta \cdot \gamma \cdot M}{1 + \zeta^*/w_{\max}} \cdot \exp(-d_{\max}^2).$$

Subtracting and using $1/(1 + \zeta^*/w_{\max}) \leq 1$ and $d_{\min} < d_{\max}$:

$$\begin{aligned} \Delta_w &\geq \delta \cdot \gamma \cdot M \cdot \exp(-d_{\min}^2) - \frac{\delta \cdot \gamma \cdot M}{1 + \zeta^*/w_{\max}} \exp(-d_{\max}^2) \\ &\geq \frac{\delta \cdot \gamma \cdot M}{1 + \zeta^*/w_{\max}} [\exp(-d_{\min}^2) - \exp(-d_{\max}^2)], \end{aligned}$$

establishing (6). ■

Corollary 1.1. Under the conditions of Theorem 1, \mathcal{X}^* achieves strictly lower \mathcal{S}_w and strictly lower semantic error than \mathcal{X}_{QAM} , while exhibiting strictly higher average BER.

Proof: The \mathcal{S}_w reduction follows from Theorem 1. The average BER increases because the descent direction that reduces \mathcal{S}_w crowds low-SCI symbols into high-density interior regions, increasing their individual error probability. Since these errors fall on semantically negligible symbols, the semantic error decreases simultaneously. ■

V. SIMULATION RESULTS AND ANALYSIS

We evaluate the proposed system on MNIST, Fashion-MNIST, and the Free Spoken Digit Dataset (FSDD), spanning basic image classification, complex visual feature extraction, and audio processing to demonstrate its cross-domain multimodal capability. All neural networks are implemented in TensorFlow and trained on an NVIDIA DGX Spark server, with the PHY simulated using the GPU-accelerated Sionna PHY library [14]. To facilitate reproducibility, the complete source code are publicly available at ¹. The wireless channel is modeled as AWGN, evaluated over $[-10, 20]$ dB SNR. Modulation orders span $M \in \{4, 16, 64, 256, 1024\}$, with the

¹<https://github.com/THE-TRAIN-LAB/Semantic-QAM>

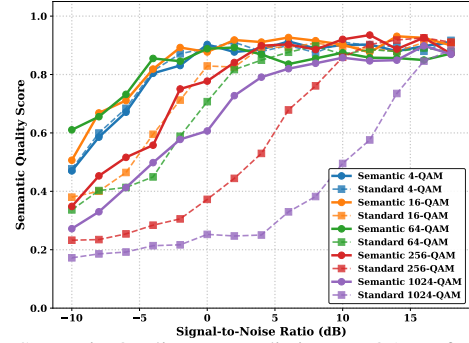


Fig. 3: Semantic Quality across distinct M-QAMs for MNIST.

codebook size constrained to $|\mathcal{C}| = M$ in each configuration. All numeric hyperparameters are listed in Table I. The *standard M-QAM* baseline retains the SC pipeline but uses a fixed rectangular grid instead of a learned constellation. The composite semantic quality score is defined as: $\mathcal{Q}_{\text{sem}} = 0.6 Q_{\text{task}} + 0.25 P_c + 0.15 \exp(-D_{\text{KL}}(p||\hat{p}))$, where Q_{task} is strict classification accuracy, $P_c = 1 - \mathbb{E}[|\max(p) - \max(\hat{p})|]$ measures how faithfully the peak classifier confidence is preserved, where p and \hat{p} are the softmax output distributions of \mathcal{T} evaluated on the original and reconstructed images respectively. $\exp(-D_{\text{KL}}(p||\hat{p}))$ measures distribution similarity using KL divergence D_{KL} . The weighting prioritizes strict task accuracy over classifier output distribution fidelity.

A. Semantic Quality and the BER Paradox

Fig. 3 compares \mathcal{Q}_{sem} across all modulation orders for the MNIST dataset. Semantic M -QAM consistently outperforms standard M -QAM across the full SNR range, with average gains of approximately 40% at low SNR (-10 to 0 dB) and 15% at high SNR (5 to 15 dB), with the gap widening at higher modulation orders where Semantic 1024-QAM achieves $\mathcal{Q}_{\text{sem}} \approx 0.60$ versus 0.25 for its standard counterpart at 0 dB. This demonstrates that the learned constellation maintains task accuracy even at low-SNR regime by ensuring high SCI concepts are well separated from others. The narrower gain at $M = 4$ is a direct consequence of the codebook constraint: with only 4 concepts, the SCI cannot finely decouple task-critical features from background noise.

Fig. 4 shows that semantic M -QAM exhibits strictly *higher* average BER at higher SNR than Standard M -QAM across all modulation orders. This is because the learned mapper deliberately crowds low-SCI symbols into the centre of the I/Q plane, sacrificing their decodability to maximize physical separation for task-critical concepts. Since these bit-level errors fall entirely on semantically negligible symbols, they have near-zero impact on \mathcal{Q}_{sem} . This empirically validates Corollary 1.1.

B. Adaptive Compression and Latency

Fig. 5 shows that the DRL agent scales K inversely with SNR, using larger K for redundancy at low SNR and aggressive Top- K compression at high SNR. Even at -10 dB, semantic 1024-QAM transmits fewer than 40 symbols per image versus 627 in the baseline ($> 15\times$ reduction), exceeding $20\times$ at high SNR. This demonstrates that joint

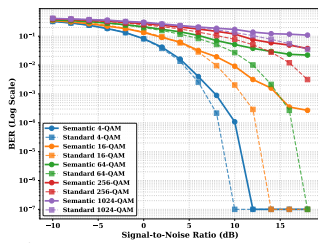


Fig. 4: Bit Error Rate vs. SNR (dB).

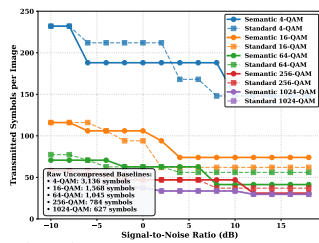
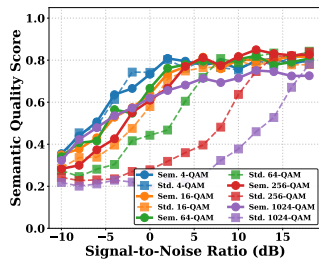
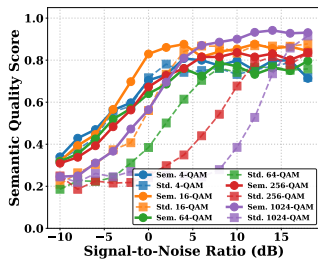


Fig. 5: Symbols transmitted vs. SNR.



(a)

(b)

Fig. 6: Semantic Quality vs. SNR (dB) for FSDD audio (a) and Fashion-MNIST visual (b) datasets.

semantic compression and PHY protection improves \mathcal{Q}_{sem} while reducing symbol count across all SNRs.

C. Cross-Domain Generalization

The system’s cross-domain applicability is validated on the Fashion-MNIST visual dataset [15] and the audio-based FSDD dataset, where semantics are extracted from audio spectrograms. Fig. 6 shows that the semantic constellation consistently outperforms the standard baseline across all modulation orders and SNR regimes. The adaptive compression and BER paradox behaviors remain consistent across modalities, indicating that the semantic constellation architecture is robust and dataset-agnostic.

D. Semantic Symbol Vulnerability Analysis

In Fig. 7, the left panel colours each learned 256-QAM symbol by its average SCI. The right panel maps the \mathcal{S}_w onto the same constellation. Two protection strategies emerge. High-SCI symbols with large $|\mathcal{N}_i|$ are pushed to the outer perimeter, maximizing physical distance from their co-occurring neighbors (*spatial isolation*). Conversely, several high-SCI symbols reside safely in the dense interior, where their vulnerability is negligible because $P(i, j) \approx 0$ for all physical neighbors j (*probabilistic isolation*). This behavior is precisely the mechanism characterized by the stationarity condition in (7) and cannot emerge from any importance-blind assignment, including Gray-coded QAM. Fig. 8 confirms that the semantic constellation consistently suppresses \mathcal{S}_w across all modulation orders, with the gap growing with M as predicted by (6), while maintaining near 100% \mathcal{S}_p versus roughly 50% for standard constellations at $M = 1024$.

VI. CONCLUSION

In this paper, we have introduced a novel semantic QAM architecture that prioritizes the physical-layer protection of task-critical features. By leveraging a DRL-based rate controller and an SCI-weighted loss function, the proposed system natively isolates highly semantic concepts from channel noise. Empirical evaluations across visual and acoustic datasets

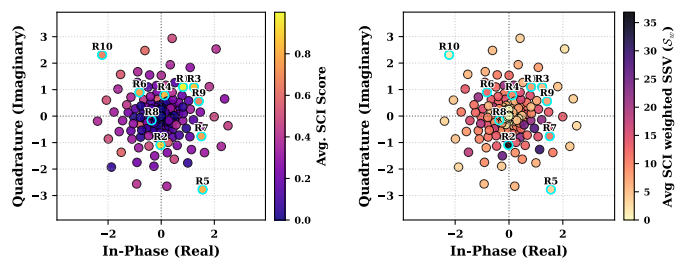
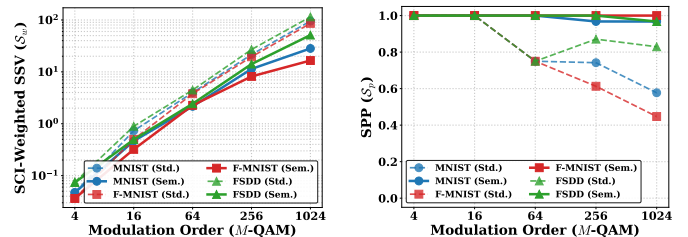


Fig. 7: Learned 256-QAM constellation with respect to (a) average SCI and (b) \mathcal{S}_w . Cyan rings highlight the top-10 most critical concepts (R1–R10).



(a) \mathcal{S}_w vs. M -QAM

(b) \mathcal{S}_p vs. M -QAM

Fig. 8: SSV and SPP analysis across modulation orders.

confirm that our approach maintains near 100% protection for critical symbols and achieves massive compression gains over standard baselines, even in severely degraded SNR regimes. This framework offers a robust, scalable foundation for next-generation AI-native 6G networks.

REFERENCES

- [1] C. E. Shannon, “A mathematical theory of communication,” *The Bell System Technical Journal*, vol. 27, no. 3, pp. 379–423, 1948.
- [2] M. Kountouris and N. Pappas, “Semantics-empowered communication for networked intelligent systems,” *IEEE Communications Magazine*, vol. 59, no. 6, pp. 96–102, 2021.
- [3] C. Chaccour, W. Saad, M. Debbah, Z. Han, and H. V. Poor, “Less data, more knowledge: Building next-generation semantic communication networks,” *IEEE Communications Surveys & Tutorials*, vol. 27, no. 1, pp. 37–76, 2024.
- [4] A. van den Oord, O. Vinyals, and K. Kavukcuoglu, “Neural discrete representation learning,” in *Advances in Neural Information Processing Systems*, 2017, vol. 30.
- [5] T. O’Shea and J. Hoydis, “An introduction to deep learning for the physical layer,” *IEEE Transactions on Cognitive Communications and Networking*, vol. 3, no. 4, pp. 563–575, 2017.
- [6] M. Stark, F. Ait Aoudia, and J. Hoydis, “Joint learning of geometric and probabilistic constellation shaping,” in *Proceedings of the 2019 IEEE Global Communications Conference Workshops (GC Wkshps)*, dec 2019, pp. 1–6.
- [7] Tung Y. Tung, David B. Kurka, Mayo Jankowski, and Deniz Gündüz, “DeepJSCC-Q: Constellation constrained deep joint source–channel coding,” *IEEE Journal on Selected Areas in Information Theory*, vol. 3, no. 4, pp. 720–731, 2022.
- [8] L. Wang, W. Wu, F. Zhou, Z. Yang, Z. Qin, and Q. Wu, “Adaptive resource allocation for semantic communication networks,” *IEEE Transactions on Communications*, vol. 72, no. 11, pp. 6900–6916, 2024.
- [9] J. Park, W. S. Ko, J. Choi, S.-L. Kim, and M. Bennis, “Towards semantic communication protocols for 6g: From protocol learning to language-oriented approaches,” *arXiv preprint arXiv:2310.09506*, 2023.
- [10] J. Shao, Y. Mao, and J. Zhang, “Learning task-oriented communication for edge inference: An information bottleneck approach,” *IEEE Journal on Selected Areas in Communications*, vol. 40, no. 1, pp. 197–211, 2021.
- [11] X. Zhan, J. Cao, X. Zhu, N. Pappas, Z. Qin, and S. Feng, “Toward robust semantic communications: Proactive importance-ordered restructuring for enhanced unequal error protection,” *arXiv preprint arXiv:2604.00595*, 2026.
- [12] A.J. Goldsmith and S.G. Chua, “Adaptive coded modulation for fading channels,” *IEEE Trans. Commun.*, vol. 46, no. 5, 1998.
- [13] Y. Bengio, N. Léonard, and A. Courville, “Estimating or propagating gradients through stochastic neurons for conditional computation,” *arXiv preprint arXiv:1308.3432*, 2013.
- [14] J. Hoydis, S. Cammerer, F. A. Aoudia, A. Vem, N. Binder, G. Marcus, and A. Keller, “Sionna: An open-source library for next-generation physical layer research,” *arXiv preprint arXiv:2203.11854*, 2022.

- [15] H. Xiao, K. Rasul, and R. Vollgraf, "Fashion-mnist: a novel image dataset for benchmarking machine learning algorithms," *arXiv preprint arXiv:1708.07747*, 2017.